A simple and industrially scalable method for making a PANI-modified cellulose touch sensor

Graphical abstract

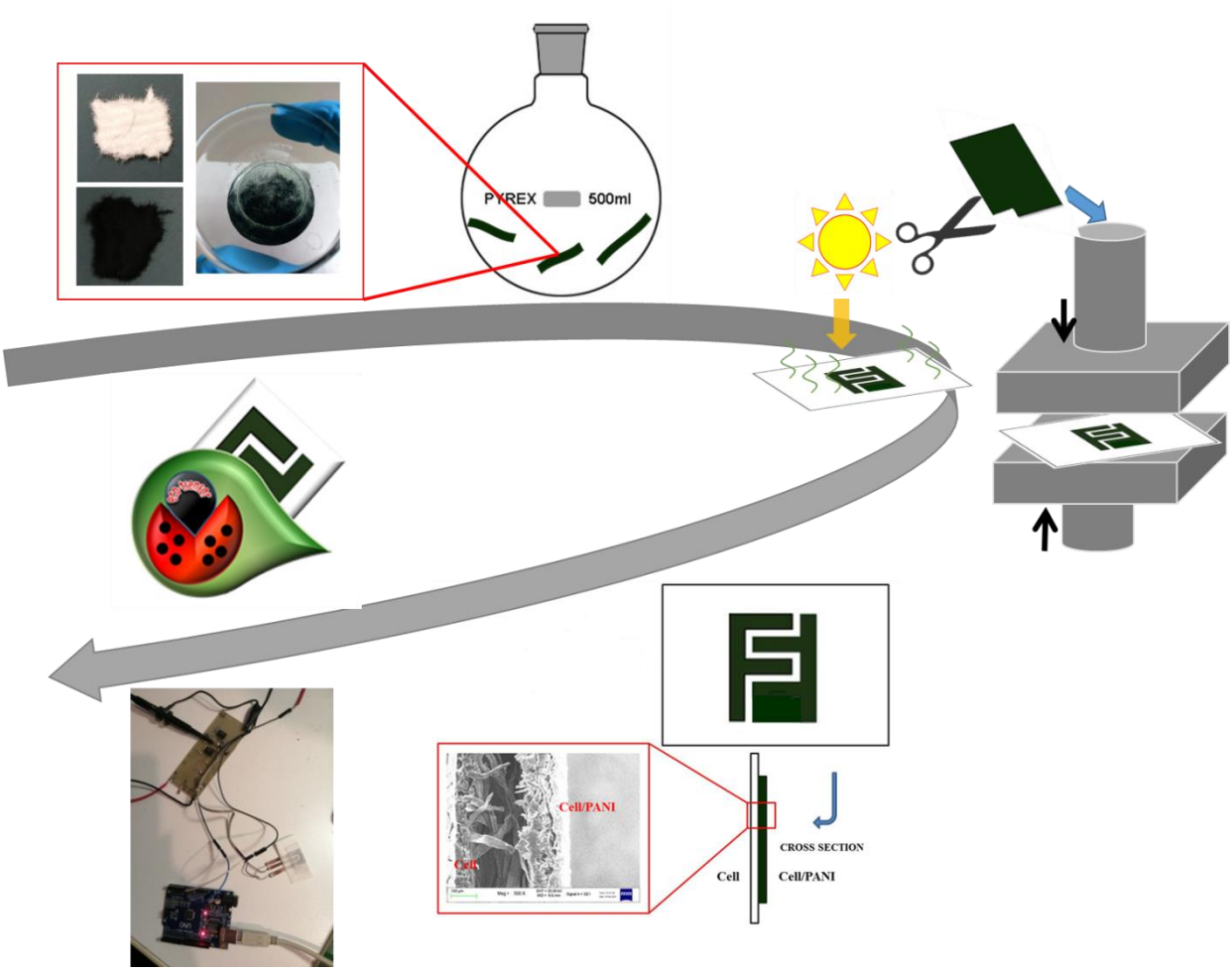

A simple and industrially scalable method for making a PANI-modified cellulose touch sensor

I. Ragazzini[a], I. Gualandi[a*], S. Selli[b], C. Polizzi[a], M. C. Cassani[a], D. Nanni[a], F. Gambassi[a], D. Tonelli[a], E. Scavetta[a], B. Ballarin[a*]

[a]Department of Industrial Chemistry "Toso Montanari", Bologna University, Via Risorgimento 4, I-40136, Bologna, Italy.

[b] Cromatos s.r.l., via G. Cardano, 6B/C/D – 47122 Forlì, Italy.

*To whom correspondence should be addressed. E-mail: barbara.ballarin@unibo.it (B.B), tel: +39 051 2093700; isacco.gualandi2@unibo.it (I.G.), tel: +39 051 2093386.

Abstract

In this work we present a simple, inexpensive, and easily scalable industrial paper process to prepare sheets of conductive cellulose fibers coated with polyanilines. First, bare fibers were coated by in situ oxidative polymerization of polyaniline then, the resulting composite fibers were used to fabricate electroactive sheets. The resistivity of the sheets is 14 ± 1 Ω sq^{-1}, a value around 1000 times lower than those reported in literature. The superior electronic proprieties of the sheets were demonstrated by assembling a capacitive touch sensor device with optimized geometry. The touch sensor shows an increase of 3-4 % of the starting electric capacity after compression and a fast response time of 52 ms. To our knowledge this is the first time that a device is prepared in this way and therefore, the herein presented results can bring an significant improvement in the development of low-cost, green and high-tech electronic devices.

Keywords: electro-active paper; PANI; cellulose; transducers; touch sensor

1. INTRODUCTION

In the current world, many action is eased by the presence of electrical devices but only 20% of these appliances is correctly recycled. Many landfills continue to be stuffed with unwanted electronics and workers are exposed to hazardous and carcinogenic substances during informally recycling processes in developing countries. As new products are consumed by hungry customers wanting the latest and greatest technology, the sheer volume of these daily produced discarded materials makes this task apparently insurmountable (EU Report).

Research efforts are focused on the development of an alternative to traditional electronics that should be low-cost, degradable, compostable, and made from environmentally nontoxic substances. As a candidate, cellulose is one of the most investigated raw materials, mainly because of high abundance on Earth, biocompatibility, porosity, high flexibility and light-weight (Khan, Abas, Kim, & Kim, 2016) (Luo & Huang, 2014). In addition, its low price (about 0.1 cent dm^{-2}) (Tobjörk & Österbacka, 2011) and its recyclability make cellulose an economically very viable option (John, Mahadeva, & Kim, 2010) (Kanaparthi & Badhulika, 2017) (Tian, Qu, & Zeng, 2017). Despite its high surface resistivity at relative humidity of 20-40 % (typically 10^{11}-10^{15} Ω sq^{-1}) (Tobjörk & Österbacka, 2011), it can be used as support to produce conductive paper that can be exploited in a wide range of applications, including supercapacitors, microfluidic systems, diagnostic devices, actuators and sensors (Luo & Huang, 2014) (Kanaparthi & Badhulika, 2017) (Sanandiya, Vijay, Dimopoulou, Dritsas, & Fernandez, 2018) (Q. Wang et al., 2018).

Two different approaches to prepare conductive paper are described in literature. In the first one, organic or inorganic conductive, semi-conductive and dielectric printable materials is deposited on paper employing screen, inkjet printing or flexographic techniques (Tobjörk & Österbacka, 2011). The second approach consists in embedding conductive materials such as functionalized multi-walled carbon nanotubes, inorganic nanoparticles and conducting polymers (CPs) in cellulose fibers making them conductive (Khan et al., 2016) (Tobjörk & Österbacka, 2011) (John et al., 2010) (Yan et al.,

2016) (Pang et al., 2016) (Gu & Huang, 2013) (Rafatmah & Hemmateenejad, 2020) (Das, Mai, & Duan, 2019) (Y. Zhang et al., 2019) (Silva et al., 2019) (Sharma, Pareek, Rohan, & Kumar, 2019) (W. Zhang et al., 2019) (Zang et al., 2018). Conducting cellulosic fibers produced by coating with CPs (i.e. polyaniline (PANI), polypirrole (PPY), poly(3,4-ethylenedioxythiophene) (PEDOT) etc.) are being explored for various applications including supercapacitors, batteries, transistors, conductive wires, actuators and touch sensors (Tobjörk & Österbacka, 2011) (Aguado, Murtinho, & Valente, 2019) (Ma, Wang, & Yu, 2020).

In this scenario PANI is particularly interesting because of its low cost, easy preparation, good environmental stability and tunable electrical properties by varying its oxidation state (Tobjörk & Österbacka, 2011)(Singh & Shukla, 2020)(Yanmin Wang, Liu, Han, & Li, 2019)(Tanguy, Thompson, & Yan, 2018)(Yanmin Wang et al., 2019)(Shoaie et al., 2019). In situ polymerization is the most popular way of depositing PANI on cellulosic fibers. Different methods can be employed depending on the types of fiber, oxidants, medium, dopants, monomers, concentration used, processing steps and parameters (John et al., 2010) (Ma et al., 2020) (Singh & Shukla, 2020) (Ke et al., 2019).

Herein we first report the preparation of cellulose/PANI fibers (Cell/PANI-F) in which PANI, in the form of protonated conductive emeraldine salt, was obtained by a simple in situ oxidative polymerization of aniline on bare cellulose fibers in acidic media (Ma et al., 2020) (Ke et al., 2019) (Masood et al., 2019). Successively, the fibers were assembled to give electroactive sheets (Cell/PANI-S) with different thickness and resistivity: 1.25 mm with a resistivity of 14 ± 1 Ω sq^{-1} (0.5 S cm^{-1}) or 0.4 mm with a resistivity of 237 ± 9 Ω sq^{-1} (0.1 S cm^{-1}). Finally, differently from those reported in the literature which are normally of resistive type (Tao et al., 2017) (Shao et al., 2014), capacitive touch sensors (Cell/PANI-TS) with an optimized geometry were assembled. Both electroactive sheets and touch sensors were prepared using an industrially and easily scalable paper process provided by the industrial group Cromatos s.r.l. (https://www.cromatos.com).

The capacitive touch sensors were finally interfaced with Arduino UNO developed board to investigate their dynamic response. All the measures have been conducted at room temperature and

in natural environment humidity after that the Cell/PANI-S or the Cell/PANI-TS were subjected to air at room temperature for the time of 24 h.

2. RESULTS AND DISCUSSION

2.1. Preparation and characterization of Cell/PANI-F and Cell/PANI-S

The modification of bare cellulosic fibers with PANI was obtained via a simple in situ oxidative polymerization of aniline in acid media, as described in the experimental section (Fig. 1).

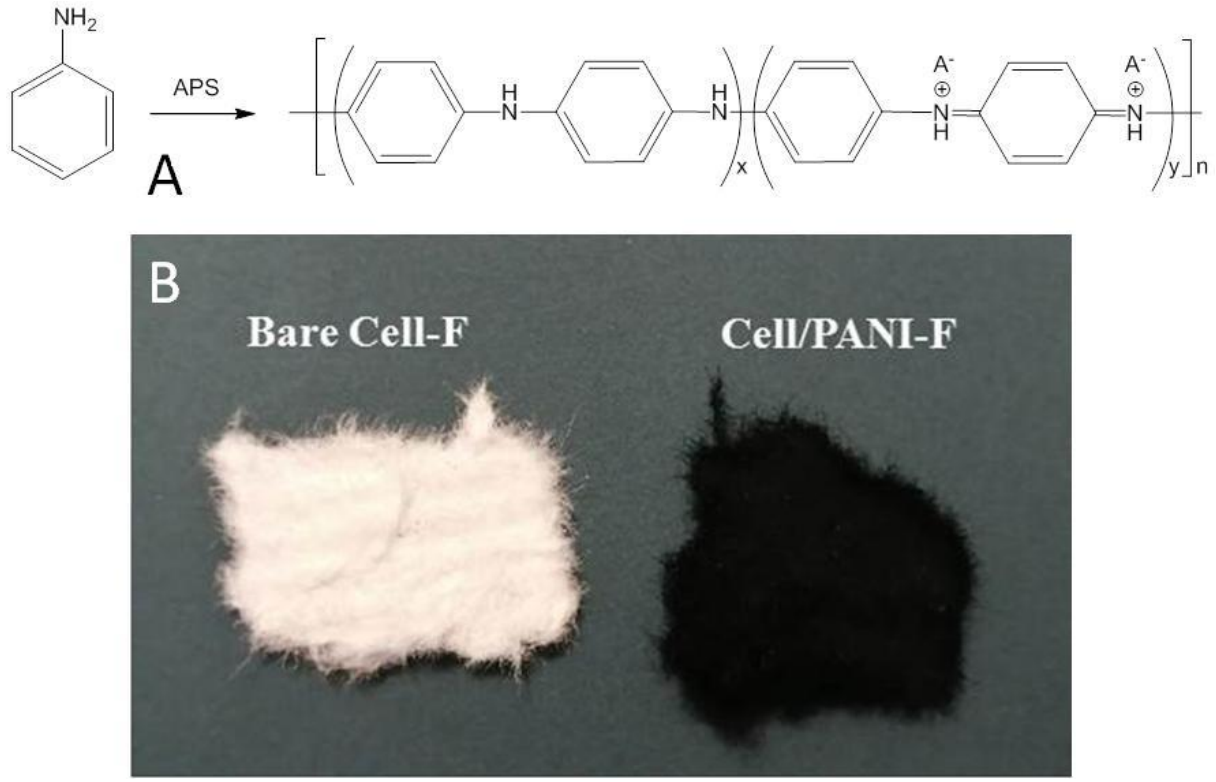

Fig. 1. A) Schematic representation of the oxidative polymerization of aniline with ammonium persulfate [$(NH_4)_2S_2O_8$, APS] in acid media; B) Image of Bare Cell-F (white) and Cell/PANI-F (black) after filtration and drying.

Scanning electron microscopy (SEM) images of bare cellulose fibers and Cell/PANI-F are reported in Fig. 2.

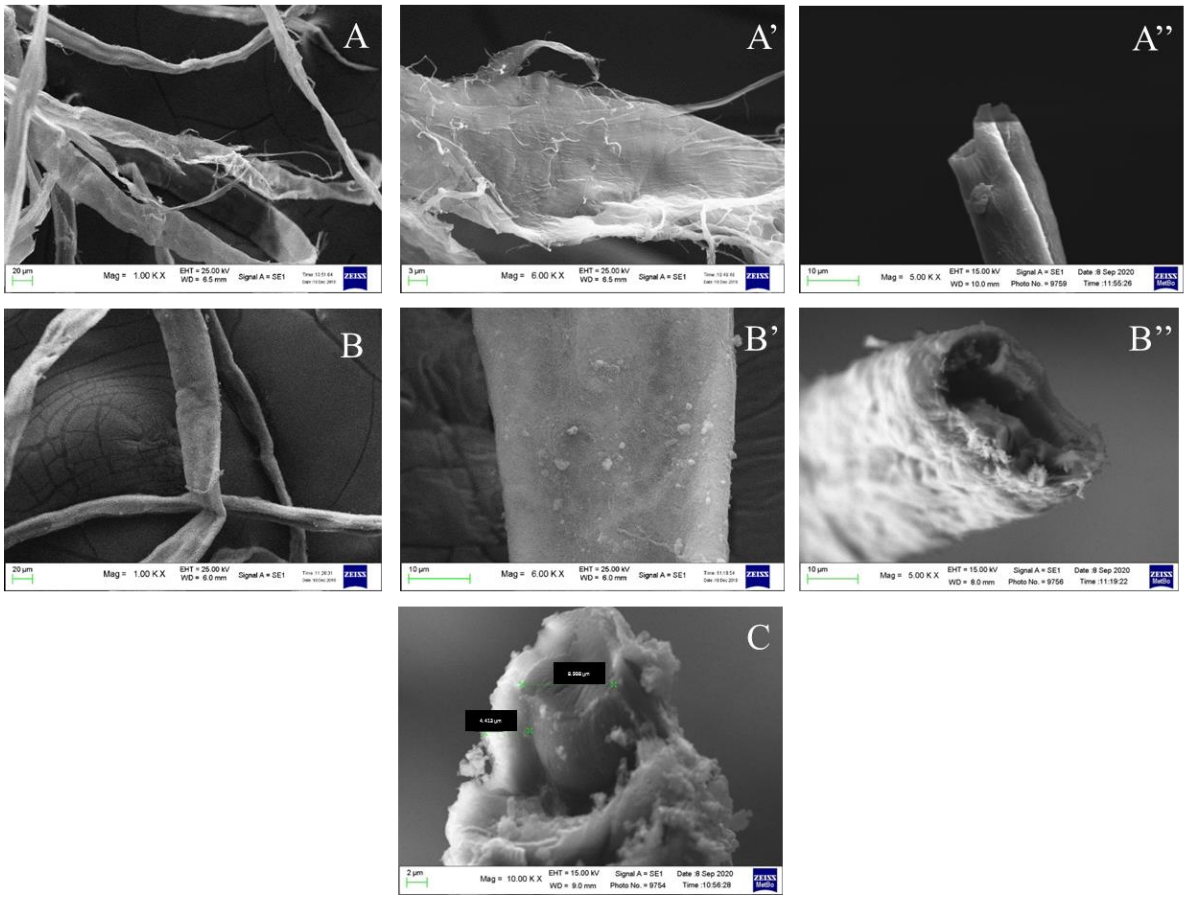

Fig. 2. Scanning electron microscopy (SEM) of bare Cell-F (A, A', A'') and Cell/PANI-F (B, B', B'') at 1000 X, 6000 X and 5000 X magnification, respectively; C) Cross-section of Cell/PANI-F at 10000 X magnification.

It can be seen from the SEM images that the pure Cell-F (Figs. 2A-A'') displayed a very clean and smooth morphology, whereas the Cell/PANI-F displayed relatively rough surface (Figs. 2B-B''). Compared the surface morphology the Cell/PANI-F is significantly different due to the deposition of PANI on the surface. All the cellulose surface results covered by a rough film that is ascribed to PANI. The PANI layer showed a relative compact morphology and well wrapped the cellulose fibers with a thickness around 4.4 μm, as observable in Fig. 2C.

SEM image and EDS element mappings of Cell/PANI-F sample are presented in Fig. 3. Within the elemental maps, the C signal originates from the cellulose fiber and PANI; O signal comes from

cellulose fiber and the N signals uniquely indicate the PANI regions. N was observed only in the outer space of cellulose fibers.

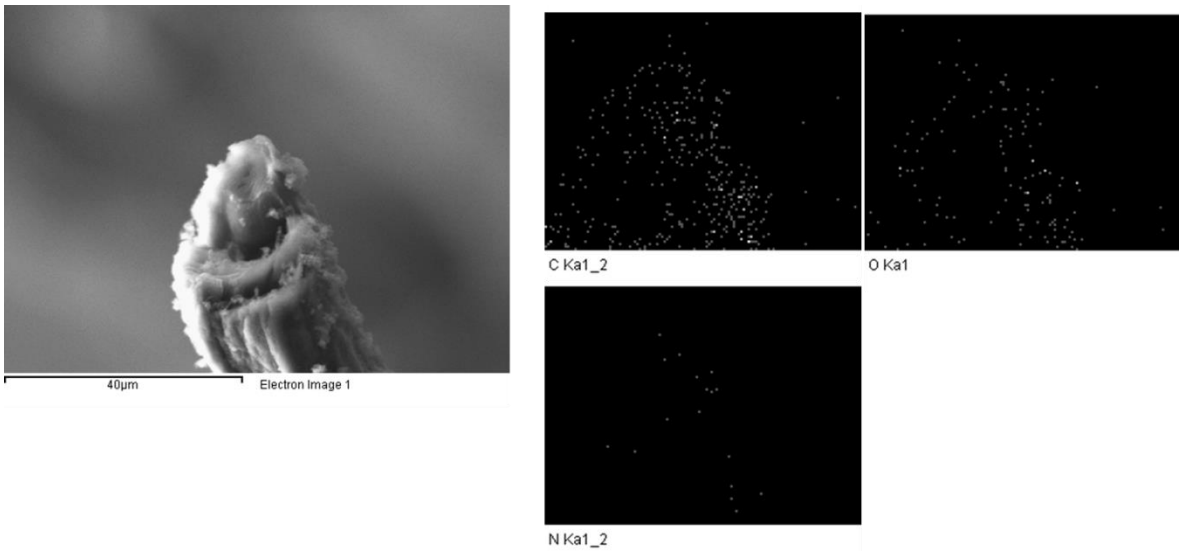

Fig. 3. EDS elemental mapping of CELL/PANI-F for Carbon, Oxygen and Nitrogen.

The PANI average amount on cellulose fibers was measured using the Kjeldahl method after digestion of the Cell/PANI-F sample and resulted 22.3 wt%.

The conductive sheets Cell/PANI-S were prepared from the Cell/PANI-F, using a protocol commonly employed for coloring paper with acid dyes (Supplementary Information, SI and Scheme S1) (Cartari, 2003). In order to maintain the polyaniline in the oxidized state (emeraldine salt), the modified fibers were immersed in a 25% $Al_2(SO_4)_3$ aqueous solution kept at *ca.* pH 3.0. Successively, after being partially dried in a square sieve and kept in a press at 50 bar for 10 s, sheets of 200 grams for square meter (200 gsm) and a thickness of 0.40 mm were obtained. Alternatively, thicker sheets (1.25 mm; 630 gsm) were prepared in a similar fashion.

The ATR-FTIR spectra of Cell/PANI-S (Fig. 4) show all the characteristic peaks attributed to PANI: the stretching vibrations of benzoid N-B-N and quinoid N=Q=N structures show up at 1443 and 1564 cm^{-1}, separately. The absorption band at 1290 is ascribed to protonation of PANI. Bare

cellulose shows the characteristic absorption peaks at ca. 3300 cm^{-1} attributed to the stretching of hydroxyl groups ν(-OH) and 2900 cm^{-1} attributed to the stretching of C-H groups; moreover, in the region of 1300 cm^{-1} the -OH bending and the C-O antisymmetric bridge stretching are present and the strong bands around 1000 cm^{-1} due to the C-O-C pyranose ring skeletal vibration are observed (Chougale, Thombare, Fulari, & Kadam, 2013) (Cases, Huerta, Garcés, Morallón, & Vázquez, 2001) (Liu et al., 2005) (Dhibar & Das, 2014).

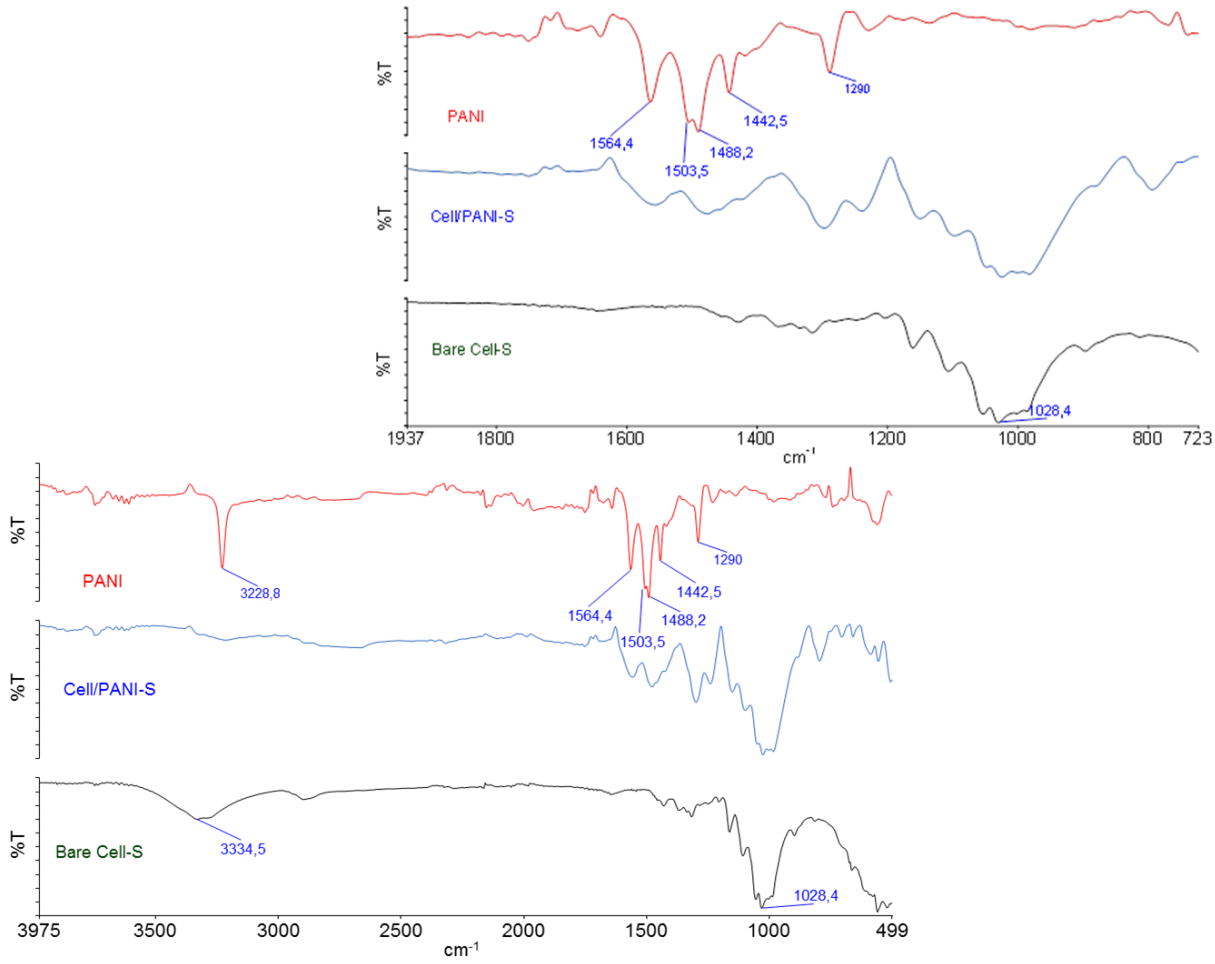

Fig. 4. ATR-FTIR spectra of bare Cellulose (black), PANI (red) and Cell/PANI-S (blue); inset: enlargement in the range 1900-700 cm^{-1}.

2.2 Cell/PANI-S electrical features

The Cell/PANI-S conductivity was evaluated by 4-line-probe measurements with a home-made sample holder (Fig. S2) to avoid the contribution due to contact resistances. In order to evaluate the reproducibility of the system, the effect of different morphology and the influence of the environmental condition during the real use, the electrical characterization was performed at different times, for each thickness, on three different paper sheets at room temperature and balanced with the surrounding atmosphere. As expected, it was found that the conductivity of Cell/PANI-S depends on the sheet thickness being 0.105 ± 0.004 S cm^{-1} for a thickness of 0.40 mm and 0.56 ± 0.06 S cm^{-1} for a thickness of 1.25 mm; in the latter the value is only one order of magnitude lower than the highest values reported for pristine PANI. It is important to underline that our preparation method allows to obtain conductivity values higher (or similar, depending from the thickness) than those achievable by all the conductive papers presented in literature, as evident from the data reported in Table 1. The small standard deviation obtained suggested the low influence of the external environmental variation (i.e. humidity).

Table 1. Comparison of the conductivity of different samples based on PANI.

Material	Synthesis	Conductivity (S cm^{-1})	Ref.
Cell/PANI-S	In situ synthesis on the cellulose pulp (1.25 mm thickness)	$5.6 \pm 0.6\ 10^{-1}$	This work
Cell/PANI-S	In situ synthesis on the cellulose pulp (0.4 mm thickness)	$1.05 \pm 0.04\ 10^{-1}$	This work
Rice pulp/PANI	In situ synthesis on the cellulose pulp	$2.5\ 10^{-5}$	(Youssef, El-Samahy, & Abdel Rehim, 2012)
Pineapple fibers/PANI	In situ synthesis on the cellulose pulp	$3.0\ 10^{-4}$	(S. I. A. Razak, N. F. A. Sharif, 2014)
Cellulose pulp/PANI	In situ synthesis on the cellulose pulp. Chemiometric optimization	$1.5\ 10^{-2}$	(Sharifi, Zabihzadeh, & Ghorbani, 2018)
CA electrospun/PANI	In situ polymerization onto electrospun cellulose membrane	$1.0\ 10^{-1}$	(Baptista et al., 2018))
Cellulose/PANI	Dispersed Cellulose + PANI	$4.7\ 10^{-8}$	(John et al., 2010)
Ink-jet printed PANI	Ink composed by PANI nanoparticles	$4.0\ 10^{-4}$	(Ngamna et al., 2007)

Thin PANI film on filter paper	In situ polymerizzation on masked paper sheet	$1.0\ 10^{-3}$	(Gao, Ota, Kiriya, Takei, & Javey, 2019)
PANI bulk		1-5	(Teo et al., 2019)

168

169 In order to clearly demonstrate the excellent conductivity of Cell/PANI-S, two 1.25 mm thick paper
170 sheets were successfully used as wires to transport the current necessary to power a LED with an
171 applied voltage of 2.0 V (Fig. 5).

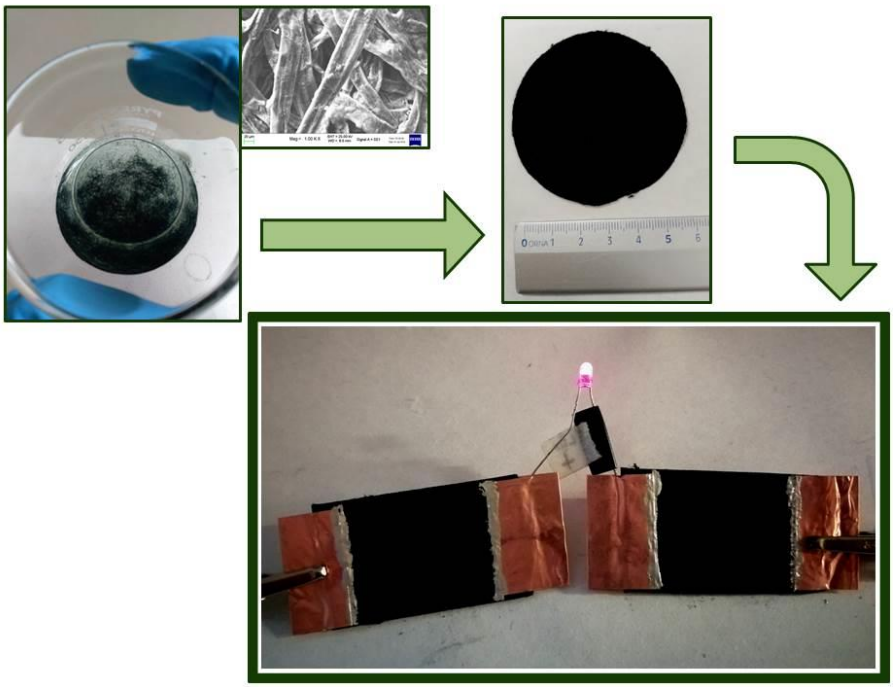

172

173 **Fig. 5.** Experimental setup with Cell/PANI-S (1.25 mm) and LED.

174

175 **2.3 Cell/PANI-TS assembling and performance**

176 Cell/PANI-TS was prepared by an industrial assembling method coupling a Cell/PANI-S (0.4 mm,
177 200 gsm) suitably cut with scissors in the required shape and a cellulose sheet (0.4 mm, 200 gsm), as
178 described in the experimental section. By maintaining the composite under a 50 bar pressure for 10

s, a device with a thickness of 0.80 mm has been obtained as reported in Figure 6 and Scheme S2. Dimensions and shape of the built circuit can be easily varied as reported in Fig. S3.

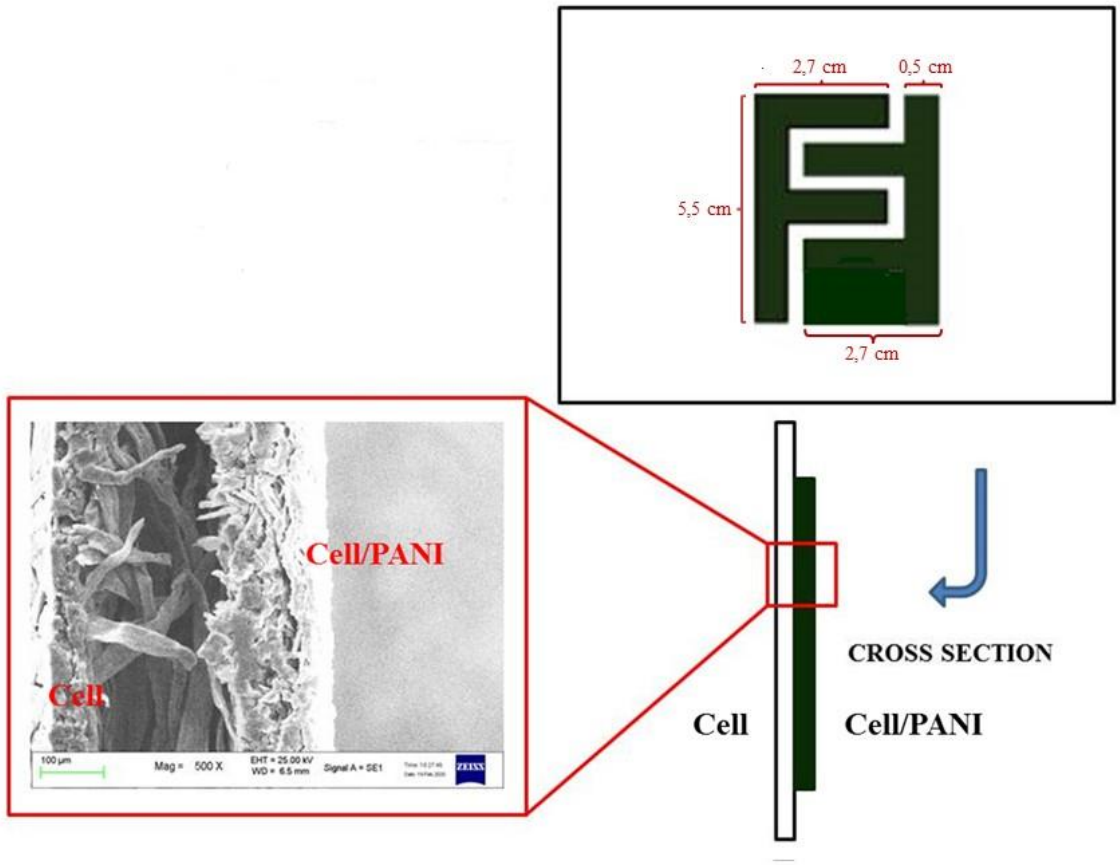

Fig. 6. Cell/PANI-TS: SEM image of the cross section and assembled circuit.

To understand the functionality of the capacitive touch sensor, an experimental test has been set up using a home-made equipment which allows to exercise and control the pressure given on the touch sensor with a step by step motor. The pressure was applied by keeping the position unchanged, and the whole area of the touch sensor was stimulated. Then the force-weight at each single advance step of the motor was measured and the capacity was recorded at the same time with Arduino UNO board (see Figs. S4-S8 and Scheme S3 for details).

Three Cell/PANI-TS samples with different geometries were tested (Fig. 7). For each, the capacitive component was measured without any touch interaction and during the dynamically induced increasing pressure up to a maximum value of 22 kPa (saturation level). The Cell/PANI-TS was excited by a square wave through the Weight Force Generator (WFG) while the out-put signal was observed with the oscilloscope and acquired with Arduino UNO development board, as described in SI. All three touch sensors have a starting capacity of about 93-94 pF and different saturation capacity depending on the geometry employed, however an increase of 3-4 % of the initial value after pressure exertion is always obtained. Fig. 7 shows the results of the tests reporting $\Delta C/C_0$ % vs pressure, where ΔC is (C_P-C_0), C_P and C_0 correspond to the capacity with and without pressure (Zang et al., 2018) (Tao et al., 2017) (Yu, Tang, Cai, Ren, & Tang, 2019) (Cataldi et al., 2018).

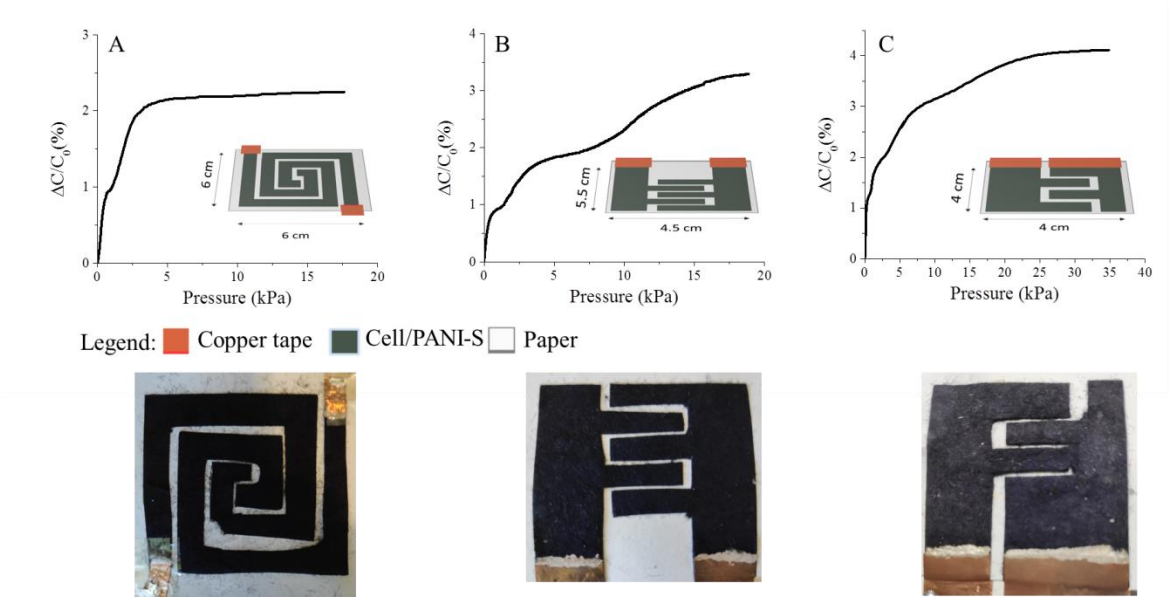

Fig. 7. Cell/PANI-TS with different geometry and related change of capacity with pressure curves.

From the data comparison, it can be observed that the geometry heavily affects the response as shown in Fig. 7. A-type sensor shows two different linear trends with a sensitivity, defined by (C_P-C_0)/C_0/P where P is the used pressure (Zang et al., 2018) (Tao et al., 2017) (Yu et al., 2019), of 0.66 kPa^{-1} in a small pressure range (0 to 2 kPa) and 0.012 kPa^{-1} in a large pressure range (2 to 20 kPa) (Figure S9). On the contrary, the C-type sensor curve follows a logarithmic trend with equation y =

0.598 ln(x) + 1.724; R^2 = 0.954 (Fig. S10) and shows sensitivities of 2.34 (0.45 σ%), 1.37 (0.44 σ%) and 0.19 (0.44 σ%) kPa^{-1} at pressures of 0.5, 2 and 20 kPa, respectively (average of five different measurements). Under each pressure both sensors display a good and stable response. Finally, B-type sensor present a different behavior which cannot be traced back to a simple mathematical expression. Due to its logarithmic behavior, we have chosen to carry out the repeatability and stability tests only on C-type sensors, recording, for each device, six independent $\Delta C/C_0$ % vs pressure curves, at different data. The results shown in Fig. S11, indicate a good reproducibility under all pressure range without a noticeable degradation of the performances.

Finally, a pressure around 6 kPa was used to examine the sensors time response revealing a response time of 52 ± 1 ms.

3. CONCLUSIONS

To the best of our knowledge, for the first time, an easily scalable industrial paper process is here proposed to produce conductive paper sheets with excellent electrical performances as demonstrated by the success of their use in the fabrication of capacitive touch sensors. This method can provide an enormous improvement in the field of low-cost electronic technology. The electroactive sheets exhibit a conductivity around five times higher than those reported in literature for similar systems and can be employed to light a LED with an applied potential of 2.0 V, highlighting the outstanding electrical performances of these composite materials. The capacitive touch sensors show a very quick response time (52 ms) and a sensibility that can be easily modulated by changing the geometry of the device.

4. EXPERIMENTAL SECTION

4.1 Materials

All chemicals and solvents are ACS reagent grade, were purchased from commercial vendors and used directly unless otherwise stated. Sulfuric acid (H_2SO_4, 95.0-98.0%), ammonium persulfate [$(NH_4)_2S_2O_8$), ≥ 98%] and aniline (≥ 99%), were purchased from Sigma-Aldrich (now Merck KGaA, Darmstadt, Germany); aniline was distilled under nitrogen prior to use. Citric acid (≥ 99.5%) was purchased from VWR Chemicals (Vienna, Austria); a solution of ca. 25 wt% of $Al_2(SO_4)_3$ in water (commercial name FLOCLINE S8C) was purchased from Bio-Line s.r.l. (Milano, Italy). Bare cellulose fibers (pine tree long fiber with sulfate treatment) were kindly provided by Cromatos s.r.l. (Forlì, Italy).

4.2 Preparation of Cell/PANI-F

In a 1 L round bottom flask, 2.5 g of bare cellulose fibers were dispersed in demineralized water (250 mL) for 30 min; successively a solution made of 2.5 mL of aniline in 150 mL of 1.0 M citric acid ($C_6H_8O_7$) was added to the fiber suspension and stirred for 3 h at room temperature. In turn, the oxidative polymerization was carried out adding dropwise to the stirred suspension, previously cooled to 0 °C in an ice bath, a solution of 7 g of $(NH_4)_2S_2O_8$ dissolved in 200 mL of 1.0 M citric acid. After 24 h the coated fibers were filtered in a Buchner funnel and washed several times with 1.0 M citric acid solution. The conductive fibers were dried in air atmosphere for 24 h; see Scheme 1 for details.

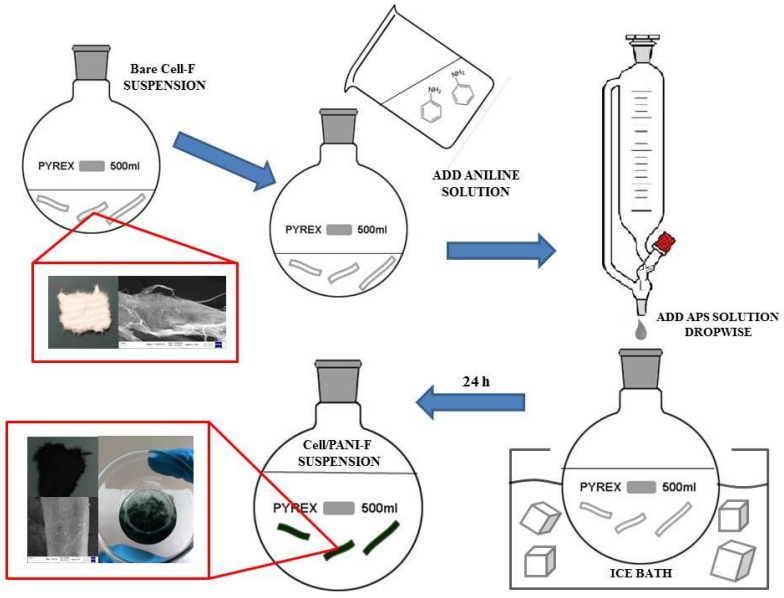

Scheme 1. Preparation steps for Cell/PANI-F.

4.3 Preparation of Cell/PANI-S

10 g of Cell/PANI-F were added to 1.0 L of an acid solution (ca. pH 3.0, 25 wt% $Al_2(SO_4)_3$ in demineralized water) and stirred for 5 min. The fibers were partially dried in a square sieve (21.0 cm x 14.8 cm size). The sheet was pressed at 50 bar pressure (P50 AXA manual hydraulic press) for 10 s to obtain the Cell/PANI-S (200 gsm, 0.40 mm thickness). Similarly, a 1.25 mm thick sheet was prepared by using 30 g of fibres (see Scheme S1 for the industrial steps details).

4.4 Preparation of Cell/PANI-TS

The wet coupling method employed in the paper industry to produce sheets of paper with variable thicknesses or with greater resistance was used to prepare the Cell/PANI-TS samples. A Cell/PANI-S of 0.40 mm thickness was cut in the desired shape and coupled with a cellulose sheet (th. 0.40 mm) moistened with water. The two sheets were then pressed (50 bar, 10 s) and dried at 80 °C for 10 min. The electrical connections were made afterwards with copper adhesive tape and silver glue, see Scheme S2 for details. The whole six-steps preparation from fibers to touch sensor is reported in Scheme 2.

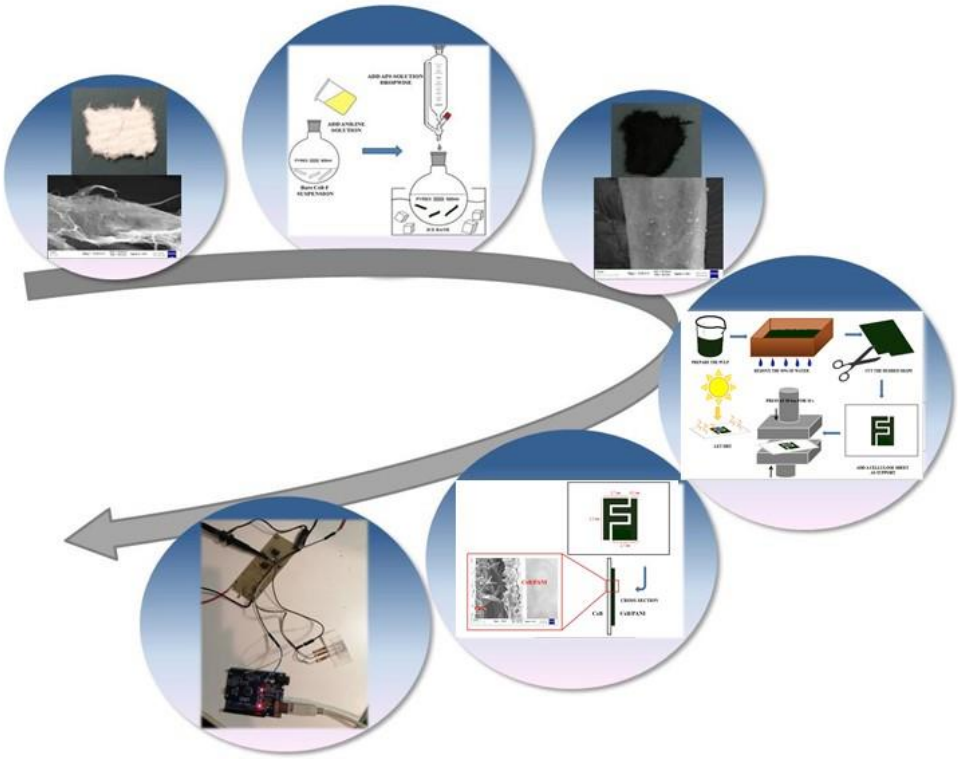

Scheme 2. Six-steps preparation for cellulose/PANI touch sensor preparation.

4.5 Instruments

ATR-FTIR analyses were performed using a Perkin Elmer Spectrum Two spectrophotometer, equipped with a Universal ATR accessory, with a resolution of 0.5 cm^{-1} in the range 4000-400 cm^{-1}. The samples were directly analyzed performing 40 scans for any analysis.

The determination of PANI amount in Cell/PANI-F was performed with an automatic Kjeldahl Nitrogen Analyzer (Gerhardt Bonn). The Kjeldahl analysis was carried out on four Cell/PANI-F samples and a blank sample (cellulose bare fibre treated exactly as the Cell/PANI-F) using the following protocol. 1.0 g of each sample was put in a glass weighing flask and placed in a Kjeldahl test tube. A catalyst tablet (1 tablet contains 3.5 g of K_2SO_4 and 3.5 mg of Se) (Kjeldahl tablets, 1.18649 Supelco, Merck), 20 mL of concentrated H_2SO_4 (sulfuric acid 95-98%, ACS reagent,

277 258105 Sigma-Aldrich) and 4 glass spheres were then added. The test tubes were heated to 350 ° C
278 for 5 h. The final solution must be clear and colourless. Finally, the test tubes were inserted in the
279 Kjeldahl titration instrument and the potentiometric titration automatically start with 0.100 M HCl in
280 presence of an acid basic indicator (a mixture of methyl red and bromocresol green).

281 SEM images were recorded at 25 kV with a Sem Zeiss EVO 50 EP equipped with Oxford
282 INCA 350; EDS Sprectrometer equipped with a Bruker Z200 energy dispersive microanalysis (EDX)
283 system was used for semi-quantitative chemical analysis and mapping.

284 ***4.6 Electrical measurements***

285 Cell/PANI-S resistance was measured with a keysight B2902A source meter units in a 4-line-
286 probe configuration by exploiting a home-made holder that is composed by 4 parallel copper
287 electrodes on a glass slide (Figure S1). The sample was prepared with a rectangular shape and was
288 held down with an insulating material by exerting a uniform pressure on all the surface. The inner
289 electrodes measure the difference of potential while a constant current flow was forced between the
290 two outer electrodes. The measurements were performed at different current values (100, 200, 300
291 µA) and a line passing from the origin was always obtained. The resistance (R) was calculated with
292 the Ohm's law and the sheet resistance ($R_{\blacksquare}$) is equal to:

293 $$R_{\blacksquare} = R\,\frac{W}{L}$$

294 Where W and L are the width and the length, respectively.

295 The specific resistance (ρ) can be calculated by:

296 $$\rho = R_{\blacksquare}\,t$$

297 Where t is the thickness. The specific conductance (κ) is calculated by:

298 $$\kappa = \frac{1}{\rho}$$

4.7 Test execution for capacitive vs pressure curves

In order to standardize the measurements, a nitrile rubber (Buna-N, Perbunan - NBR) was chosen as dielectric material and was interposed between the pressure generator and the sensor (P.Cataldi et al., 2018). The sensor was housed in the appropriate seat apparatus reported in Figure S4 and a force-weight was exerted with an increase step of 1.0 g (subsequently converted into Pascal) on the whole sensor surface and the capacity was recorded at the same time.

ASSOCIATED CONTENT

Supporting information

The Supporting Information is available free of charge on the Publication website at DOI:

AUTHOR INFORMATION

Corresponding Autors

***Barbara Ballarin,** Dipartimento di Chimica Industriale Toso Montanari, UNIBO, Viale Risorgimento 4, 40136 Bologna-IT

orcid.org/0000-0003-3698-2352; E-mail: **barbara.ballarin@unibo.it**

***Isacco Gualandi**, Dipartimento di Chimica Industriale Toso Montanari, UNIBO, Viale Risorgimento 4, 40136 Bologna-IT

orcid.org/0000-0002-6823-7501; E-mail: **isacco.gualandi2@unibo.it**

Author contributions

B.B., E.S., I.G., I.R., conceived the project, supervised the preparation and analysis of the samples, analysed the data and wrote the paper. C.P. designed and developed the electronic experiments set-up. S.S. helped to assemble the sheets and the touch sensors. M.C.C. and F.G. participated in analytical data collection and analysis. D.T. and D.N. revised the manuscript.

ACKNOWLEDGEMENTS

The authors thank the University of Bologna for financial support. The authors gratefully thank Dr. Sandra Stipa and Dr. Fabrizio Tarterini for the SEM images and Kjeldahl analyses. Finally the authors especially thank Cromatos s.r.l. and Roberto Bezzi for the sheets preparation.

REFERENCES

10° Corso di Tecnologia per Tecnici Cartari, edizione 2002/2003; Scuola Interregionale di Tecnologia per Tecnici Cartari, Via Don G. Minzoni, 50 - 37138 Verona

Aguado, R., Murtinho, D., & Valente, A. J. M. (2019). A broad overview on innovative functionalized paper solutions. *Nordic Pulp and Paper Research Journal*, *34*(4), 395–416. https://doi.org/10.1515/npprj-2019-0036

Baptista, A. C., Ropio, I., Romba, B., Nobre, J. P., Henriques, C., Silva, J. C., Ferreira, I. (2018). Cellulose-based electrospun fibers functionalized with polypyrrole and polyaniline for fully organic batteries. *Journal of Material Chemistry A, 6(1)*, 256–265. https://doi.org/10.1039/c7ta06457h

Cataldi, P.; Dussoni, S.; Ceseracciu, L.; Maggiali, M.; Natale, L.; Metta, G.; Athanassiou, A.; Bayer, I. S. (2018) Carbon nanofiber versus graphene-based stretchable capacitive touch sensors for artificial electronic skin, *Advanced Science*, *5*, 1700587-1700597.

Cases, F., Huerta, F., Garcés, P., Morallón, E., & Vázquez, J. L. (2001). Voltammetric and in situ FTIRS study of the electrochemical oxidation of aniline from aqueous solutions buffered at pH 5. *Journal of Electroanalytical Chemistry*, *501*(1–2), 186–192. https://doi.org/10.1016/S0022-

0728(00)00526-X

Chougale, U. M., Thombare, J. V., Fulari, V. J., & Kadam, A. B. (2013). Synthesis of polyaniline nanofibres by SILAR method for supercapacitor application. *2013 International Conference on Energy Efficient Technologies for Sustainability, ICEETS 2013*, (April), 1078–1083. https://doi.org/10.1109/ICEETS.2013.6533537

Cromatos s.r.l. is an industrial group operating worldwide dedicated to the production, formulation and marketing of dyes, pigments and chemical products for industry. (https://www.cromatos.com).

Das, P., Mai, V. C., & Duan, H. (2019). Flexible bioinspired ternary nanocomposites based on carboxymethyl cellulose/nanoclay/graphene oxide. *ACS Applied Polymer Materials, 1(6)*, 1505–1513. research-article. https://doi.org/10.1021/acsapm.9b00245

Dhibar, S., & Das, C. K. (2014). Silver nanoparticles decorated polyaniline/multiwalled carbon nanotubes nanocomposite for high-performance supercapacitor electrode. *Industrial and Engineering Chemistry Research*, *53*(9), 3495–3508. https://doi.org/10.1021/ie402161e

Gao, W., Ota, H., Kiriya, D., Takei, K., & Javey, A. (2019). Flexible Electronics toward Wearable Sensing. *Accounts of Chemical Research*, *52*(3), 523–533. https://doi.org/10.1021/acs.accounts.8b00500

Gu, Y., & Huang, J. (2013). Colorimetric detection of gaseous ammonia by polyaniline nanocoating of natural cellulose substances. *Colloids and Surfaces A: Physicochemical and Engineering Aspects*, *433*, 166–172. https://doi.org/10.1016/j.colsurfa.2013.05.016

John, A., Mahadeva, S. K., & Kim, J. (2010). The preparation, characterization and actuation behavior of polyaniline and cellulose blended electro-active paper. *Smart Materials and Structures*, *19*(4). https://doi.org/10.1088/0964-1726/19/4/045011

Kanaparthi, S., & Badhulika, S. (2017). Low cost, flexible and biodegradable touch sensor fabricated by solvent-free processing of graphite on cellulose paper. *Sensors and Actuators, B: Chemical*, *242*, 857–864. https://doi.org/10.1016/j.snb.2016.09.172

371 Ke, S., Ouyang, T., Zhang, K., Nong, Y., Mo, Y., Mo, Q., Cheng, F. (2019). Highly conductive
372 cellulose network/polyaniline composites prepared by wood fractionation and in situ
373 polymerization of aniline. *Macromolecular Materials and Engineering*, *304*(7), 1–10.
374 https://doi.org/10.1002/mame.201900112
375 Khan, A., Abas, Z., Kim, H. S., & Kim, J. (2016). Recent progress on cellulose-based electro-active
376 paper, its hybrid nanocomposites and applications. *Sensors (Switzerland)*, *16*(8), 1–30.
377 https://doi.org/10.3390/s16081172
378 Liu, X. X., Zhang, L., Li, Y. B., Bian, L. J., Su, Z., & Zhang, L. J. (2005). Electropolymerization of
379 aniline in aqueous solutions at pH 2 to 12. *Journal of Materials Science*, *40*(17), 4511–4515.
380 https://doi.org/10.1007/s10853-005-0854-x
381 Luo, Y., & Huang, J. (2014). Surface modification of natural cellulose substances: Toward
382 functional materials and applications. *Science China Chemistry*, *57*(12), 1672–1682.
383 https://doi.org/10.1007/s11426-014-5226-4
384 Ma, Z., Wang, W., & Yu, D. (2020). Assembled wearable mechanical sensor prepared based on
385 cotton fabric. *Journal of Materials Science*, *55*(2), 796–805. https://doi.org/10.1007/s10853-
386 019-04035-0
387 Masood, A., Shoukat, Z., Yousaf, Z., Sana, M., Faisal Iqbal, M., Rehman, A. R., Razaq, A. (2019).
388 High capacity natural fiber coated conductive and electroactive composite papers electrode for
389 energy storage applications. *Journal of Applied Polymer Science*, *136*(13), 1–6.
390 https://doi.org/10.1002/app.47282
391 Ngamna, O., Morrin, A., Killard, A. J., Moulton, S. E., Smyth, M. R., & Wallace, G. G. (2007).
392 Inkjet printable polyaniline nanoformulations. *Langmuir*, *23*(16), 8569–8574.
393 https://doi.org/10.1021/la700540g
394 Pang, Z., Yang, Z., Chen, Y., Zhang, J., Wang, Q., Huang, F., & Wei, Q. (2016). A room
395 temperature ammonia gas sensor based on cellulose/TiO_2/PANI composite nanofibers.
396 *Colloids and Surfaces A: Physicochemical and Engineering Aspects*, *494*, 248–255.

https://doi.org/10.1016/j.colsurfa.2016.01.024

Rafatmah, E., & Hemmateenejad, B. (2020). Dendrite gold nanostructures electrodeposited on paper fibers: Application to electrochemical non-enzymatic determination of glucose. *Sensors and Actuators, B: Chemical*, *304*(October 2019), 127335. https://doi.org/10.1016/j.snb.2019.127335

Razak S. I. A, Sharif, N. H. M. N. (2014). Elect rically Conductive Paper of Polyaniline Modified Pineapple Leaf Fiber. *Fibers and Polymers*, *15*, 1107. https://doi.org/10.1007/s12221-014-1107-x

Report EU. (n.d.). Retrieved from https://www.unenvironment.org/news-and-stories/press-release/un-report-time-seize-opportunity-tackle-challenge-e-waste

Sanandiya, N. D., Vijay, Y., Dimopoulou, M., Dritsas, S., & Fernandez, J. G. (2018). Large-scale additive manufacturing with bioinspired cellulosic materials. *Scientific Reports*, *8*(1), 1–8. https://doi.org/10.1038/s41598-018-26985-2

Shao, Q., Niu, Z., Hirtz, M., Jiang, L., Liu, Y., Wang, Z., & Chen, X. (2014). High-performance and tailorable pressure sensor based on ultrathin conductive polymer film. *Small*, *10*(8), 1466–1472. https://doi.org/10.1002/smll.201303601

Sharifi, H., Zabihzadeh, M., & Ghorbani, M. (2018). The application of response surface methodology on the synthesis of conductive polyaniline/cellulosic fiber nanocomposites. *Carbohydrate Polymers*, *194*(February), 384–394. https://doi.org/10.1016/j.carbpol.2018.04.083

Sharma, K., Pareek, K., Rohan, R., & Kumar, P. (2019). Flexible supercapacitor based on three-dimensional cellulose/graphite/polyaniline composite. *International Journal of Energy Research*, *43*(1), 604–611. https://doi.org/10.1002/er.4277

Shoaie, N., Daneshpour, M., Azimzadeh, M., Mahshid, S., Khoshfetrat, S. M., Jahanpeyma, F., … Foruzandeh, M. (2019). Electrochemical sensors and biosensors based on the use of polyaniline and its nanocomposites: a review on recent advances. *Microchimica Acta*, *186*(7).

https://doi.org/10.1007/s00604-019-3588-1

Silva, L. E., Cunha Claro, P. I., Sanfelice, R. C., Guimarães, M., de Oliveira, J. E., Ugucioni, J. C., Denzin Tonoli, G. H. (2019). Cellulose nanofibrils modification with polyaniline aiming at enhancing electrical properties for application in flexible electronics. *Cellulose Chemistry and Technology*, *53*(7–8), 775–786. https://doi.org/10.35812/CelluloseChemTechnol.2019.53.76

Singh, P., & Shukla, S. K. (2020). Advances in polyaniline-based nanocomposites. *Journal of Materials Science*, *55*(4), 1331–1365. https://doi.org/10.1007/s10853-019-04141-z

Tanguy, N. R., Thompson, M., & Yan, N. (2018). A review on advances in application of polyaniline for ammonia detection. *Sensors and Actuators, B: Chemical*, *257*, 1044–1064. https://doi.org/10.1016/j.snb.2017.11.008

Tao, L. Q., Zhang, K. N., Tian, H., Liu, Y., Wang, D. Y., Chen, Y. Q., Ren, T. L. (2017). Graphene-Paper Pressure Sensor for Detecting Human Motions. *ACS Nano*, *11*(9), 8790–8795. https://doi.org/10.1021/acsnano.7b02826

Teo, M. Y., Stuart, L., Devaraj, H., Liu, C. Y., Aw, K. C., & Stringer, J. (2019). The: In situ synthesis of conductive polyaniline patterns using micro-reactive inkjet printing. *Journal of Materials Chemistry C*, *7*(8), 2219–2224. https://doi.org/10.1039/c8tc06485g

Tian, Y., Qu, K., & Zeng, X. (2017). Investigation into the ring-substituted polyanilines and their application for the detection and adsorption of sulfur dioxide. *Sensors and Actuators, B: Chemical*, *249*, 423–430. https://doi.org/10.1016/j.snb.2017.04.057

Tobjörk, D., & Österbacka, R. (2011). Paper electronics. *Advanced Materials*, *23*(17), 1935–1961. https://doi.org/10.1002/adma.201004692

Wang, Q., Sun, J., Yao, Q., Ji, C., Liu, J., & Zhu, Q. (2018). 3D printing with cellulose materials. *Cellulose*, *25*(8), 4275–4301. https://doi.org/10.1007/s10570-018-1888-y

Wang, Yanhu, Zhang, L., Zhao, P., Ge, S., Yan, M., & Yu, J. (2019). Visual distance readout to display the level of energy generation in paper-based biofuel cells: application to enzymatic sensing of glucose. *Microchimica Acta*, *186*(5). https://doi.org/10.1007/s00604-019-3374-0

449 Wang, Yanmin, Liu, A., Han, Y., & Li, T. (2019). Sensors based on conductive polymers and their
450 composites: a review. *Polymer International*, (September 2019).
451 https://doi.org/10.1002/pi.5907
452 Yan, H., Guo, Y., Lai, S., Sun, X., Niu, Z., & Wan, P. (2016). Flexible Room-Temperature Gas
453 Sensors of Nanocomposite Network-Coated Papers. *ChemistrySelect*, *1*(11), 2816–2820.
454 https://doi.org/10.1002/slct.201600648
455 Youssef, A. M., El-Samahy, M. A., & Abdel Rehim, M. H. (2012). Preparation of conductive paper
456 composites based on natural cellulosic fibers for packaging applications. *Carbohydrate*
457 *Polymers*, *89*(4), 1027–1032. https://doi.org/10.1016/j.carbpol.2012.03.044
458 Yu, Z., Tang, Y., Cai, G., Ren, R., & Tang, D. (2019). Paper Electrode-Based Flexible Pressure
459 Sensor for Point-of-Care Immunoassay with Digital Multimeter. *Analytical Chemistry*, *91*(2),
460 1222–1226. https://doi.org/10.1021/acs.analchem.8b04635
461 Zang, X., Jiang, Y., Wang, X., Wang, X., Ji, J., & Xue, M. (2018). Highly sensitive pressure
462 sensors based on conducting polymer-coated paper. *Sensors and Actuators, B: Chemical*,
463 *273*(July), 1195–1201. https://doi.org/10.1016/j.snb.2018.06.132
464 Zhang, W., Wu, Z., Hu, J., Cao, Y., Guo, J., Long, M., … Jia, D. (2019). Flexible chemiresistive
465 sensor of polyaniline coated filter paper prepared by spraying for fast and non-contact
466 detection of nitroaromatic explosives. *Sensors and Actuators B: Chemical*, 127233.
467 https://doi.org/10.1016/j.snb.2019.127233
468 Zhang, Y., Yang, Z., Yu, Y., Wen, B., Liu, Y., & Qiu, M. (2019). Tunable electromagnetic
469 interference shielding ability in a one-dimensional bagasse fiber/polyaniline heterostructure.
470 *ACS Applied Polymer Materials*, *1*(4), 737–745. https://doi.org/10.1021/acsapm.8b00025
471